Application of regional meteorology and air quality models based on MIPS and LoongArch CPU Platforms

Zehua Bai[1,2], Qizhong Wu[1,2], Kai Cao[1,2], Yiming Sun[3], Huaqiong Cheng[1,2]

[1]College of Global Change and Earth System Science, Faculty of Geographical Science, Beijing Normal University, Beijing 100875, China.

[2]Joint Center for Earth System Modeling and High Performance Computing, Beijing Normal University, Beijing 100875, China.

[3]Beijing Institute of Talent Development Strategy, Beijing 100032, China.

Correspondence: Qizhong Wu (wqizhong@bnu.edu.cn)

Abstract. The Microprocessor without interlocked piped stages (MIPS) and LoongArch are Reduced Instruction Set Computing (RISC) processor architectures, which have advantages in terms of energy consumption and efficiency. There are few studies on the application of MIPS and LoongArch CPUs in the geoscientific numerical models. In this study, Loongson 3A4000 CPU platform with MIPS64 architecture and Loongson 3A6000 CPU platform with LoongArch architecture were used to establish the runtime environment for the air quality modelling system Weather Research and Forecasting–Comprehensive Air Quality Model with extensions (WRF-CAMx) in Beijing-Tianjin-Hebei region. The results show that the relative errors for the major species (NO_2, SO_2, O_3, CO, PNO_3 and PSO_4) between the MIPS and X86 benchmark platform are within ±0.1%. The maximum Mean Absolute Error (MAE) of major species ranged to 10^{-2} ppbV or μg m^{-3}, the maximum Root Mean Square Error (RMSE) ranged to 10^{-1} ppbV or μg m^{-3}, and the Mean Absolute Percentage Error (MAPE) remained within 0.5%. The CAMx takes about 195 minutes on Loongson 3A4000 CPU, 71 minutes on Loongson 3A6000 CPU and 66 minutes on Intel Xeon E5-2697 v4 CPU, when simulating a 24h-case with four parallel processes using MPICH. As a result, the

single-core computing capability of Loongson 3A4000 CPU for the WRF-CAMx modeling system is about one-third of Intel Xeon E5-2697 v4 CPU and Loongson 3A6000 CPU is slightly lower than Intel Xeon E5-2697 v4 CPU, but the thermal design power (TDP) of Loongson 3A4000 is 40W, while the Loongson 3A6000 is 38W, only about one-fourth of Intel Xeon E5-2697 v4, whose TDP is 145W. The results also verify the feasibility of cross-platform porting and the scientific usability of the ported model. This study provides a technical foundation for the porting and optimization of numerical models based on MIPS, LoongArch or other RISC platforms.

1 Introduction

In the recent years, with the increasing demand for high-performance computing resources and rapid development in the computer industry, especially supercomputer, central processing unit (CPU) has undergone significant advancements in logical structure, operational efficiency, and functional capabilities, making it the core component of current computer technology development. There are two main types: one is complex instruction set computer (CISC) CPU (George, 1990; Shi, 2008), mainly using X86 architecture, representative vendors including Intel, AMD, etc., and widely used in high-performance computing platforms. The other is reduced instruction set computer (RISC) CPU (Mallach, 1991; Liu et al.,2022), mainly using ARM, MIPS, RISC-V and other architectures, representative vendors including Loongson, etc., and mainly used in high-performance computing platforms, which have high efficiency, excellent stability and scalability. The Microprocessor without interlocked piped stages (MIPS) architecture is one of the significant representatives of RISC architecture. MIPS was originally developed in the early 1980s by Professor Hennessy at Stanford University and his group (Hennessy et al., 1982). The simplicity of the MIPS instruction set contributes to its ability to process instructions quickly, thus achieving higher performance even in low-power conditions. In 1999, MIPS Technology Inc. released the MIPS32 and MIPS64 architecture standard (MIPS Technology Inc., 2014). Compared to the CISC CPUs, RISC CPUs demonstrate excellent performance and power efficiency, which have gained popularity among chip manufacturers.

The Loongson processor family developed by Loongson Technology is mainly designed using MIPS architecture and Linux operating system (Hu et al, 2011), which has rich application tools in Linux open-source projects. The main reason that currently restricts the development of CPUs that implement non-X86 instruction set architecture such as MIPS64 is the immature software ecosystem (Hu et al., 2016). Based on the strategy of open-source software, Loongson platform has gained abundant software tools, making it possible to further develop scientific computing and numerical models.

Air quality model (AQM) systems use mathematical equations and algorithms to simulate and predict the pollutant concentration in the atmosphere. The current AQMs have become more complex, incorporating numerous factors such as emissions from industrial sources, vehicle traffic, and natural sources, as well as meteorological conditions, including modeling meteorology, emissions, chemical reactions, and removal processes (Zhang et al., 2012). Regional-scale AQMs have been widely used to predict air quality in cities, formulate emission reduction strategies, and evaluate the effectiveness of control polices (Wang et al., 2023), including the Community Multiscale Air Quality (CMAQ) modelling system (Appel et al., 2017; Appel et al., 2021), the Comprehensive Air Quality Model with extensions (CAMx; RAMBOLL ENVIRON Inc., 2014), and the Nested Air Quality Prediction Modeling System (Wang et al., 2006; Chen et al., 2015). Due to the requirement of meteorological input, commonly used offline meteorological models such as WRF (Michalakes et al., 2001) are coupled offline with the regional AQMs to provide meteorological and chemical forecast as the WRF-AQM modeling system, such the WRF-CMAQ modeling system (Wu et al., 2014).

Both the meteorological and air quality numerical simulation rely heavily on high-performance computing systems. The WRF-AQM systems can run stably on high-performance computing platforms based on X86 or X86-compatible instruction set architecture (ISA) CPUs, which account for the highest percentage among the main processors of current high performance computing platforms. There are relatively limited researches on the application of WRF-AQM system on MIPS and LoongArch

CPU platforms at present, this study focuses on the application of WRF-CAMx model on Loongson CPU platform based on the MIPS and LoongArch architectures. A simulation case covering the Beijing-Tianjin-Hebei region was set up to evaluate the differences and performance between MIPS and X86 platforms. This study validated the stability of scientific computing on MIPS and LoongArch CPU platform, and it offered technical references and evaluation methods for the porting and application of numerical models on non-X86 platforms.

Section 2 provides the model descriptions of the Weather Research and Forecasting–Comprehensive Air Quality Model with extensions (WRF-CAMx) modeling system, and the descriptions of MIPS, LoongArch and benchmark platforms. The configuration of the air quality numerical simulation system and simulation case are also presented in Section 2. Section 3 describes porting and optimization of the WRF-CAMx modelling system on MIPS and LoongArch CPU platforms. Section 4 analyzes the differences of model results between MIPS CPU platform and the benchmark platform. Section 5 discusses MIPS and LoongArch CPUs performance in scientific computing. The conclusions are presented in Section 6.

2 Model and Porting Platform Description

The air quality modeling system was constructed using the WRF v4.0 model developed by National Center for Atmospheric Research (NCAR) (Skamarock et al., 2019), and the CAMx v6.10 developed by Ramboll Environment (RAMBOLL ENVIRON Inc., 2014), as shown in Figure 1. And the Loongson 3A4000 CPU platform was chosen for the porting work in the study. This study introduced the porting of WRF-CAMx modeling system to MIPS and LoongArch CPU platforms.

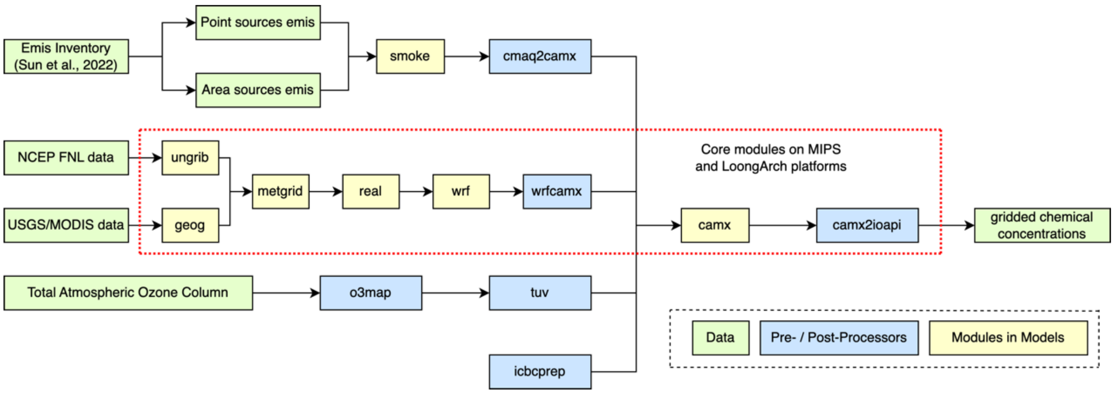

Figure 1. Framework of WRF-CAMx modeling system. The core modules have been ported to MIPS and LoongArch CPU platforms. The core modules are framed by red dashed line in the figure.

In Xi'an, China and Milan, Italy, the WRF-CAMx modelling system was applied , enabling high-resolution hourly model output of pollutant concentration within specific local urban areas (Pepe et al., 2016; Yang et al., 2020). The modeling system is widely used to study the spatial-temporal variation of pollutant concentration and source apportionment, analyze the contribution of regional transport to pollution and investigate the impact of initial conditions and emissions on pollution simulation in key regions such as the North China Plain, Sichuan Basin, and Fenwei Plain (Bai et al., 2021; Zhen et al., 2023; Zhang et al., 2022; Xiao et al., 2021).

2.1 Description of WRF-CAMx modeling system

WRF and CAMx serve as the core components of the modeling system. WRF is a mesoscale numerical weather prediction system designed for atmospheric research and operational forecasting applications. Distinguished by its high temporal and spatial resolution, WRF is suitable for multi-scale simulations of short-term weather forecast, atmospheric process, and long-term climate, making it an essential tool in the meteorological and atmospheric research communities (Powers et al., 2017). In the modeling system, WRF provided gridded meteorological field data for air quality model CAMx. The relative humidity, a meteorological variable used in result validation is calculated using the wrf-python package (Official website: https://wrf-python.readthedocs.io, last access: October 2023). CAMx is an atmospheric pollutant calculation model, which can be utilized for simulating and predicting the concentrations of various air pollutants. The WRF and CAMx models are distinguished by modularity and parallelism, using MPI in parallel computing, making them efficient (Skamarock et al., 2019; RAMBOLL ENVIRON Inc., 2014).

In the modeling system, the SMOKE model and cmaq2camx program are used to process emission data and provide model-ready gridded emission data for the CAMx model. The wrfcamx program converts the WRF results into meteorological input files which are compatible with CAMx. TUV is a radiation transfer model capable of producing clean sky photolysis rate input files for the chemical mechanisms in CAMx, and the o3map program prepares ozone column input files for TUV and CAMx. The icbcprep program prepares initial and boundary condition files for CAMx with the profile, and the effects of initial conditions have been studied by Xiao et al. (2021). The camx2ioapi program converts the CAMx output files into netCDF format following the Models-3/IO-API convention, and then uses NCL or other softwares to analyses the model results.

2.1.1 Model domain setup

The model domain focusing on the Beijing-Tianjin-Hebei region has been set up in this study. The WRF model has three nested domains with horizontal resolutions of 27km (D1), 9km (D2), and 3km (D3), as shown in Figure 2. The outer domain (D1) covers most parts of China, and the inner domain (D3) covers Beijing, Tianjin, and Hebei Province. The model domain is centered at (35°N, 110°E), with two true latitudes located at 20°N and 50°N. The vertical resolution of WRF is 34 vertical layers. The CAMx model has only one model domain, which is the innermost grid with a resolution of 3km (D3), mainly covering the Beijing-Tianjin-Hebei region. The vertical resolution of CAMx is 14 vertical layers, which is extracted from the WRF output files using the wrfcamx module, and the lower seven layers of CAMx are same as those in the WRF model.

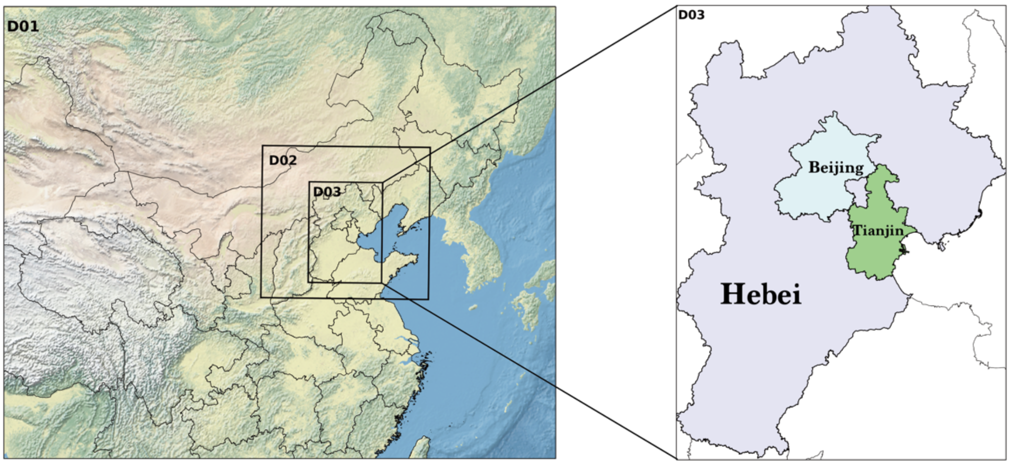

Figure 2. The domains of three-level nested grids in the WRF-CAMx modelling system. The respective horizontal resolutions are 27 km × 27 km (D1), 9 km × 9 km (D2), and 3 km × 3 km (D3).

2.1.2 Model configuration

Starting from 00:00 on November 3, 2020, until 24:00 on November 5, 2020, the modelling system simulated the meteorological and air quality for a period of 72 hours. In the research of Wang et al. in 2019, a 72h test case was set for the scientific validation and performance evaluation of the chemistry transport models. A 72h case represents a moderate-sized real scientific workload, which allows for simulating in a short time to validate the results and assess computational efficiency on the MIPS and LoongArch platforms. For the meteorological model, the global meteorological initial and boundary fields for the WRF model are derived from the NCEP Global Final Reanalysis Data (FNL), with a spatial resolution of 0.5° x 0.5° and a temporal resolution of 6 hours. And the parameterization schemes of the WRF model used in the simulation case are shown in Table 1.

For the air quality model, the meteorological files are provided by the WRF model are used for the chemical transport module in CAMx. The emission inventory used in the simulation case was obtained from Sun et al. (2022a). It contains basic emissions from Sun et al. (2022b) and fugitive dust emission from bare ground surfaces. The SMOKE model (v2.4) is used to process the emission inventory and provide gridded emissions for CAMx. The parameterization schemes of the CAMx model used in the simulation case are shown in Table 2.

Table 1. Parameterization schemes of WRF in research case.

Parameterization process	Scheme
Microphysics	WSM3
Longwave radiation	RRTM
Shortwave radiation	Dudhia
Land surface	Noah
Planetary boundary layer	YSU
Cumulus parameterization	Kain-Fritsch(new Eta)

Table 2. Parameterization schemes of CAMx in research case.

Parameterization process	Scheme
Horizontal Diffusion	PPM
Vertical Diffusion	K-theory
Dry Deposition	Zhang03
Gas-phase chemical mechanism	CB05
Aqueous aerosol chemistry	RADM-AQ
Inorganic gas-aerosol partitioning	ISORROPIA

2.1.3 Statistical indicators for model results

To quantify the differences in the model results between the MIPS and benchmark platform, three statistical indicators are used to analyze the differences of concentration time series: Mean Absolute Error (MAE), Root Mean Square Error (RMSE), and Mean Absolute Percentage Error (MAPE). The MAPE quantifies the deviation between computational differences and simulated values. The smaller these indicators, the better accuracy and stability of scientific computing of the modeling system on the MIPS platform. The calculation formulas for these statistical indicators are provided in equations (1) to (3).

$$MAE = \frac{1}{n}\sum_{i=1}^{n}\left|MIPS(i) - Base(i)\right| \quad (1)$$

$$RMSE = \left[\frac{1}{n}\sum_{i=1}^{n}\left(MIPS(i) - Base(i)\right)^2\right]^{\frac{1}{2}} \quad (2)$$

$$MAPE = \frac{1}{n}\sum_{i=1}^{n}\left|\frac{MIPS(i)-Base(i)}{MIPS(i)}\right| \times 100\% \quad (3)$$

In the equations, *n* represents the number of grids in the domain. *MIPS(i)* represents the simulated value of a certain grid on the MIPS platform, and *Base(i)* represents the baseline value of a certain grid on the benchmark platform.

2.2 MIPS and LoongArch CPU platforms description

Loongson CPU platform was chosen for the porting work in the study. Currently, the Loongson processor family has three generations of CPU products, evolving from single-core to multi-cores architectures and from experimental prototypes to mass-produced industrial products (Hu et al., 2011). The Loongson-2 processor is a 64-bit general-purpose RISC processor series which is compatible with MIPS instruction set. It can be used in personal computers, mobile terminals, and various embedded applications, running many operating systems such as Linux and Android smoothly (Zhi et al., 2012). Wu et al. (2019) reports the application of the mesoscale model on Loongson 2F CPU platform. The Loongson-3 processor features a scalable multi-core architecture, targeting high-throughput data centers, high-performance scientific computing, and other applications, with the significant advantage of achieving a high peak performance-to-power ratio and striking a well-balanced trade-off between performance and power consumption (Hu et al., 2009).

The Loongson 3A series are multi-core processors designed for high-performance computers, featuring with high bandwidth, and low power consumption. The efficient design solution and the advantage of high energy efficiency ratio make servers based on Loongson CPUs highly competitive in performance, power consumption, and cost-effectiveness (Li et al., 2014; Wang et al., 2014). In this study, the Loongson platform uses the Debian Linux operating system, commercially known as Tongxin UOS (https://www.uniontech.com, last access: January, 2024), and the Loongson 3A4000 processor, which is the first quad-core processor based on GS464v 64-bit microarchitecture in Loongson 3 Processor Family. The main technical parameters of Loongson 3A4000 CPU are shown in Table 3. Compared to previously released CPUs, the processor improves frequency and performance by optimizing on-chip interconnect and memory access path, integrating 64-bit DDR4 memory controller and on-chip security mechanism. The Loongson 3A6000 CPU platform uses Loongnix, the open-source community edition operating system released by Loongson (https://www.loongson.cn/system/loongnix, last access: January, 2024), and the latest released Loongson 3A46000 processor, which is a quad-core processor based on LA664 microarchitecture. The main technical parameters of Loongson 3A6000 CPU are shown in Table 3. The processor supports the LoongArch™ instruction set and hyper-threading, and the performance has significantly improved compared to the previously released processors (Hu et al., 2022).

Table 3. Main Parameters of Loongson 3A4000 CPU and Loongson 3A6000 CPU[*]

Main Parameters	Loongson 3A4000 CPU	Loongson 3A6000 CPU
Main Frequency	1.8GHz–2.0GHz	2.0GHz–2.5GHz
Peak Computing Speed	128Gflops@2.0GHz	240Gflops
Transistor Technology	28nm	12nm
Number of Cores	4	4(Physical) 8(Logical)
Processor Cores	MIPS64 compatible Support 128/256-bit vector instructions	support LoongArch™ Support 128/256-bit vector instructions
High-speed I/O	2 x 16-bit HyperTransport 3.0 control	1 x HyperTransport 3.0 control
Typical Power Consumption	<30W@1.5GHz <40W@1.8GHz <50W@2.0GHz	38W@2.5GHz

[*]source: https://www.loongson.cn, last access: January, 2024.

2.3 Benchmark platform description

This study uses an X86 CPU platform as benchmark platform compared to the MIPS and LoongArch CPU platforms. The benchmark platform is powered by Intel Xeon E5-2697 v4 CPU, with strong floating-point performance and many technical features such as Intel Turbo Boost Technology (Intel Inc., 2023). The Intel Xeon E5-2697 v4 CPU has 18 cores, with 2.3GHz base frequency and 3.6GHz maximum Turbo Boost frequency, 45 MB Intel Smart Cache and 145W design power consumption. The operating system is CentOS Linux 7.4.1708. The main information for all platforms is shown in Table 4.

Table 4. The comparison of main configuration between MIPS, LoongArch and X86 platforms.

	MIPS Platform	**LoongArch Paltform**	**X86 platform**
CPU	Loongson 3A4000	Loongson 3A6000	Intel Xeon E5-2697 v4
Number of CPUs	1	1	1
Number of CPU cores	4	8	18
CPU Frequency	1.8GHz	2.0Ghz	2.3GHz
CPU instruction set	MIPS64	LoongArch™	X86_64
Operating system	Tongxin UOS	Loongnix	CentOS Linux 7.4.1708
Operating system kernel (Linux version)	4.19.0-loongson-3-desktop	4.19.0-19-loongson-3	3.10.0-957.1.3.el7.x86_64

2.4 The difference between MIPS, LoongArch and X86 platforms

In this study, the numerical model's source code is written in Fortran, and commonly used compilers for X86 architecture include Intel Compiler, PGI and GNU Compiler. The compiler for MIPS platform is built using GCC 8.3 MIPS GNU/Linux cross-toolchain based on the open-source GNU Project, called MIPS GNU, and the latest version is 8.3. And the compiler for LoongArch platform is built using GCC 8.3 LoongArch GNU/Linux cross-toolchain based on the open-source GNU Project, called LoongArch GNU, and the latest version is 8.3. The compiler for the benchmark platform is set to X86 GNU, and the version is also 8.3. Table 5 shows the differences between all platforms' GNU compilers in terms of applicable platforms. Compared to X86 GNU, the default compilation options of MIPS GNU compiler not only specify the platform architecture but also include additional instruction sets, such as atomic operation instruction set LLSC, shared library instruction set PLT, etc., which can optimize target programs compiled by GNU for MIPS architecture and improve computational efficiency. And the default compilation options of LoongArch GNU compiler not only specify the platform architecture but also include target microarchitecture tuning option, which can also optimize target programs compiled by GNU for LoongArch architecture.

Table 5. Comparison of GNU compiler between MIPS, LoongArch and X86 CPU platforms.

Artitecture	**MIPS64**	**LoongArch**	**x86_64**
Compiler	MIPS GNU Fortran	LoongArch GNU Fortran	X86 GNU Fortran
Version	8.3	8.3	8.3
Target	mips64el-linux-gnuabi64	loongarch64-linux-gnu	x86_64-redhat-linux
Options (Architecture)	-march=mips64r2 -mabi=64	-march=loongarch64 -mabi=lp64d	-march=x86-64 -mtune=generic
Options (Instruction set)	-mllsc -mplt -mmadd4	-mtune=loongarch64	/
FLAGS(WRF)	-fconvert=big-endian -frecord-marker=4 -ffree-line-length-none -O2 -ftree-vectorize -funroll-loops		
FLAGS(CAMx)	-fconvert=big-endian -frecord-marker=4 -ffixed-line-length-none -fno-align-commons -O2		

The WRF-CAMx modeling system depends on several scientific computing libraries. Firstly, the general data format libraries netCDF and HDF5 are required to store the large-scale gridded data for the modeling system. NetCDF is a self-describing data format developed by NCAR/Unidata, primarily used for storing multidimensional array data in fields like meteorology and earth sciences (UCAR/Unidata, 2021). HDF5 is a data format developed by HDF GROUP that supports complex data structures with multiple data types and multi-dimensional datasets (The HDF Group, 2019). In this study, netCDF-C (v4.8.1), netCDF-Fortran (v4.5.3), HDF5 (v1.12.1) and IOAPI (v3.1) were successfully installed on MIPS and LoongArch platforms by building from their sources, which are obtained from the official website.

The MPICH library is required to support parallel computing in the modeling system. In order to fully utilize computing resources, the method of MPI message communication is used in WRF and CAMx model (Wu et al., 2012). MPICH is an open-source, portable parallel computing library for implementing the MPI standard (Amer et al., 2021). It supports inter-process communication and data exchange in the parallel computing environment. Similarly, this study successfully installed MPICH (v3.4) on MIPS and LoongArch platforms by building from its source. During the compilation and installation of the mentioned libraries above, the configure tool was used to check the basic information of the platform's CPU and compiler, and prepare for compatibility with platform before compilation, the GNU compiler is used to compile the source code of libraries, and the cmake tool is used to install the libraries. Additionally, the same runtime environment as MIPS platform was also built on the benchmark platform.

3 Porting the WRF-CAMx modelling system on MIPS and LoongArch CPU platforms

The simulation result is influenced by several factors including processor architecture, operating system, compiler, parallel environment, and scientific computing libraries. In order to ensure stability and accuracy of numerical simulation, the models should be adapted to the new runtime environment when porting across platforms. Additionally, various operating systems have different tools, software and libraries, which may impact the results of numerical simulations.

In this study, the runtime environment for WRF-CAMx modeling system was built on MIPS and LoongArch platforms, including parallel computing libraries such as MPICH3 (v3.4) and data format libraries such as HDF5 (v1.15.1) and NETCDF (C-v4.8.1, Fortran-v4.5.3). These libraries do not support the architecture (mips64el and LoongArch) and GNU compiler of Loongson platform. Relevant information needs to be added to the free software config.guess and config.sub provided by GNU org. Part of the information is shown in subfigure a) in Figure 3, which can help identify the platform architecture and system during the compilation and installation of libraries using Configure and Make tools. The configuration files for making the models were modified to fit the compilers of the Linux system on MIPS and LoongArch platforms. In order to verify the stability of scientific computing on MIPS and LoongArch platforms, a control experiment was set up on the benchmark platform, minimizing the impact of other factors on simulation results of both platforms.

The WRF v4.0 and CAMx v6.10 were successfully deployed on MIPS and LoongArch platforms through source code compilation and installation. In the WRF model, the default options for GNU compiler which are suitable for MIPS and LoongArch architecture CPUs are not provided in the configure file of the source code package, and it is necessary to incorporate architecture-specific settings for the model. For example, the architecture presets are stored in the configure.defaults file, but seetings about the Loongson platform is not included. Specific architecture details, including CPU architecture, GNU compiler and compilation flags, need to be added, which can ensure the correct display of configuration during building WRF model, and part of information is shown in subfigure b) in Figure 3. Table 5 provides the detailed information added in the configure file, mainly about MIPS and LoongArch GNU Fortran. When compiling Fortran programs on MIPS and LoongArch platforms, the MIPS and LoongArch GNU Fortran and necessary compilation flags must be specified. These flags include common Fortran file format flags such as -fconvert=big-endian and -frecord-marker=4, as well as optimization flags such as -O2 -ftree-vectorize -funroll-loops. By specifying the appropriate compiler and flags for MIPS an LoongArch architectures, the configure tool will provide necessary settings to compile WRF. Correspondingly, when compiling WRF on the benchmark platform, the compilation flags are strictly consistent with those of MIPS and LoongArch CPU platforms, which ensures that differences in simulation results of two platforms are primarily attributed to the underlying hardware architecture rather than changes in compilation settings.

In the CAMx model, the makefile provides information about parallelism and compilers. Similarly, information about the CPU architecture, GNU compiler, and compilation flags on MIPS and LoongArch platforms also needs to be added in the makefile. For the detailed information added in the makefile, please refer to Table 5. Additionally, the code of CAMx was modified to make it run smoothly on MIPs and

LoongArch platform. Taking some function in the CAMx model for example, the model frequently uses the “write” function for formatted output. The format specifiers in the parameters consist of data types (I, F, E, A, X, etc.) followed by a character width. In the CAMx model, the format specifiers in the write function mostly default to character width, but there is a compilation issue with MIPS GNU, requiring character width descriptors. It is also essential to ensure consistency with the default precision. A specific example is illustrated in the figure below. A specific example is showed in in subfigure c) in Figure 3. So far, the WRF-CAMx model has been successfully compiled and installed on the MIPS and LoongArch platforms after modifications of the configuration files mentioned above.

a)

```
,,
loongarch32:Linux:*:* | loongarch64:Linux:*:*)
    GUESS=$UNAME_MACHINE-unknown-linux-$LIBC
    ;;
    ..
mips64el:Linux:*:*)
    GUESS=$UNAME_MACHINE-unknown-linux-$LIBC
    ;;
```

b)

```
#ARCH    Linux mips64, gfortran compiler with gcc  #serial smpar dmpar dm+sm
#
DESCRIPTION     =       GNU ($SFC/$SCC)
DMPARALLEL      =       # 1
OMPCPP          =       # -D_OPENMP
OMP             =       # -fopenmp
OMPCC           =       # -fopenmp
SFC             =       gfortran
SCC             =       gcc
CCOMP           =       gcc
DM_FC           =       mpif90 -f90=$(SFC)
DM_CC           =       mpicc -cc=$(SCC)
FC              =       CONFIGURE_FC
CC              =       CONFIGURE_CC
LD              =       $(FC)
RWORDSIZE       =       CONFIGURE_RWORDSIZE
PROMOTION       =       #-fdefault-real-8
ARCH_LOCAL      =       -DNONSTANDARD_SYSTEM_SUBR  -DWRF_USE_CLM
CFLAGS_LOCAL    =       -w -O3 -c
LDFLAGS_LOCAL   =
CPLUSPLUSLIB    =
ESMF_LDFLAG     =       $(CPLUSPLUSLIB)
FCOPTIM         =       -O2 -ftree-vectorize -funroll-loops
FCREDUCEDOPT    =       $(FCOPTIM)
FCNOOPT         =       -O0
```

c)

```
Before modification:
      write (iout,'(a,2a)') ' spec','total [ug/m3]','c* [ug/m3]   '
      write (iout,'(i5,2e)') (idx(i),sctot(i),scsat(i),i=1,nsol)
      write (iout,'(a,2e)') ' cpre,cpx ',cpre,cpx
After modification:
      write (iout,'(a5,2a15)') ' spec','total [ug/m3]','c* [ug/m3]   '
      write (iout,'(i5,2e15.7)') (idx(i),sctot(i),scsat(i),i=1,nsol)
      write (iout,'(a5,2e15.7)') ' cpre,cpx ',cpre,cpx
```

Figure 3. Sample codes containing configure index, architecture-specific settings and functions in the WRF-CAMx model. Panel a) provides architecture information for configuration. Panel b) shows architecture-specific settings for WRF. Panel c) illustrates the sample code of functions in the CAMx before and after modification.

4 The differences of model results on the two platforms

4.1 Validation of the spatial distribution

A 72h simulation case has been designed to test the stability and availability of the WRF-CAMx modeling system on the MIPS CPU platform in Beijing. By analyzing the differences in simulation results and computing time, the accuracy and performance of the modeling system on MIPS platform were evaluated, which further verifies the feasibility and stability of the modeling system after porting to the MIPS platform.

Common meteorological variables, including 2-meter temperature, land surface pressure, and relative humidity were selected to verify the WRF model results. Figure 4 shows the spatial distribution of the four meteorological variables after 72 hours simulation on different platforms, as well as the absolute errors (AEs). The meteorological variables from the modeling system on the different platforms exhibit a generally consistent spatial distribution in the Beijing-Tianjin-Hebei regions shown in Figure 4.

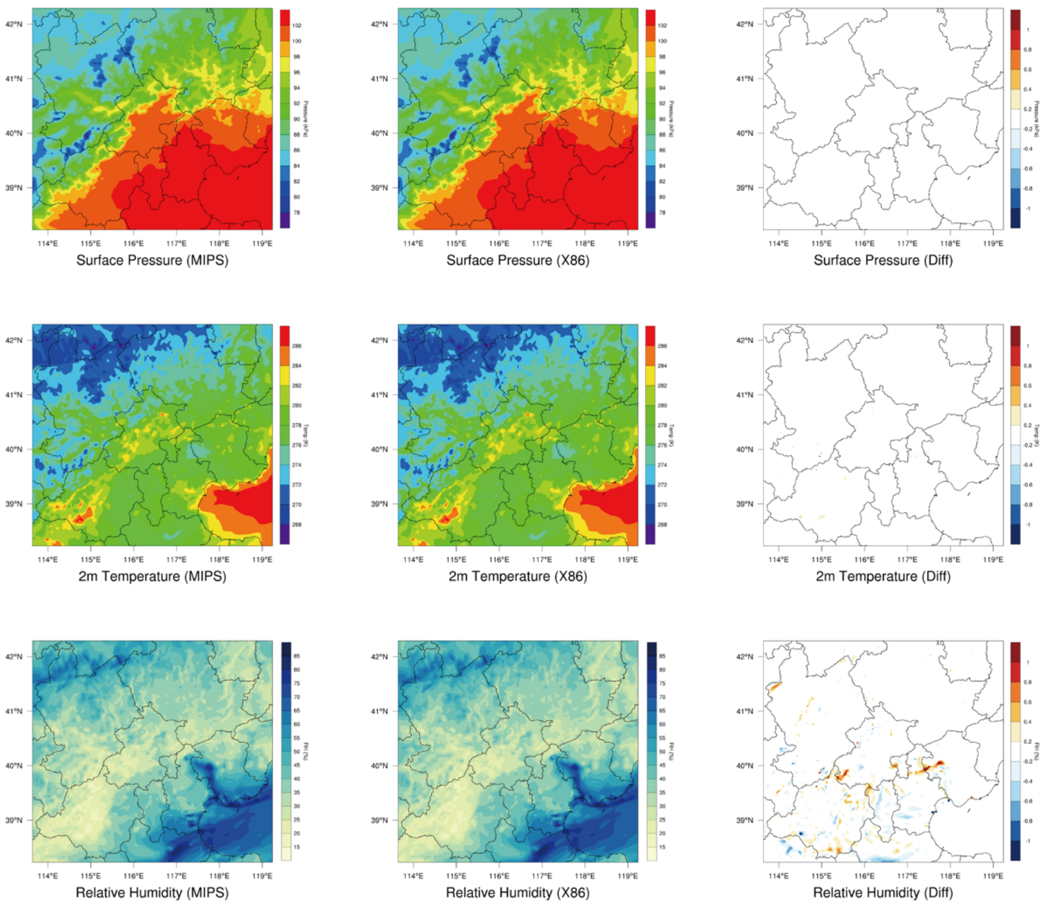

Figure 4. Spatial distribution of 2m temperature, surface pressure, relative humidity from WRF. Left column, MIPS platform. Middle, the X86 platform. Right, the differences between the MIPS and benchmark(X86) platform.

Similarly, the NO_2, SO_2, O_3, CO, PNO_3 and PSO_4 were selected to verify the

CAMx model results on the MIPS platform. Figure 5 shows the spatial distribution of the six species, as well as the absolute errors (AEs) between the two platforms after 72 hours simulation. Simulating the 72h-case with four parallel processes using MPICH, CAMx takes about 9h on Loongson 3A4000 CPU and 2.6h on Intel Xeon E5-2697 v4 CPU. As shown in Figure 5, the spatial distribution of air pollution concentrations from the different platforms is essentially consistent, appearing very similar visually.

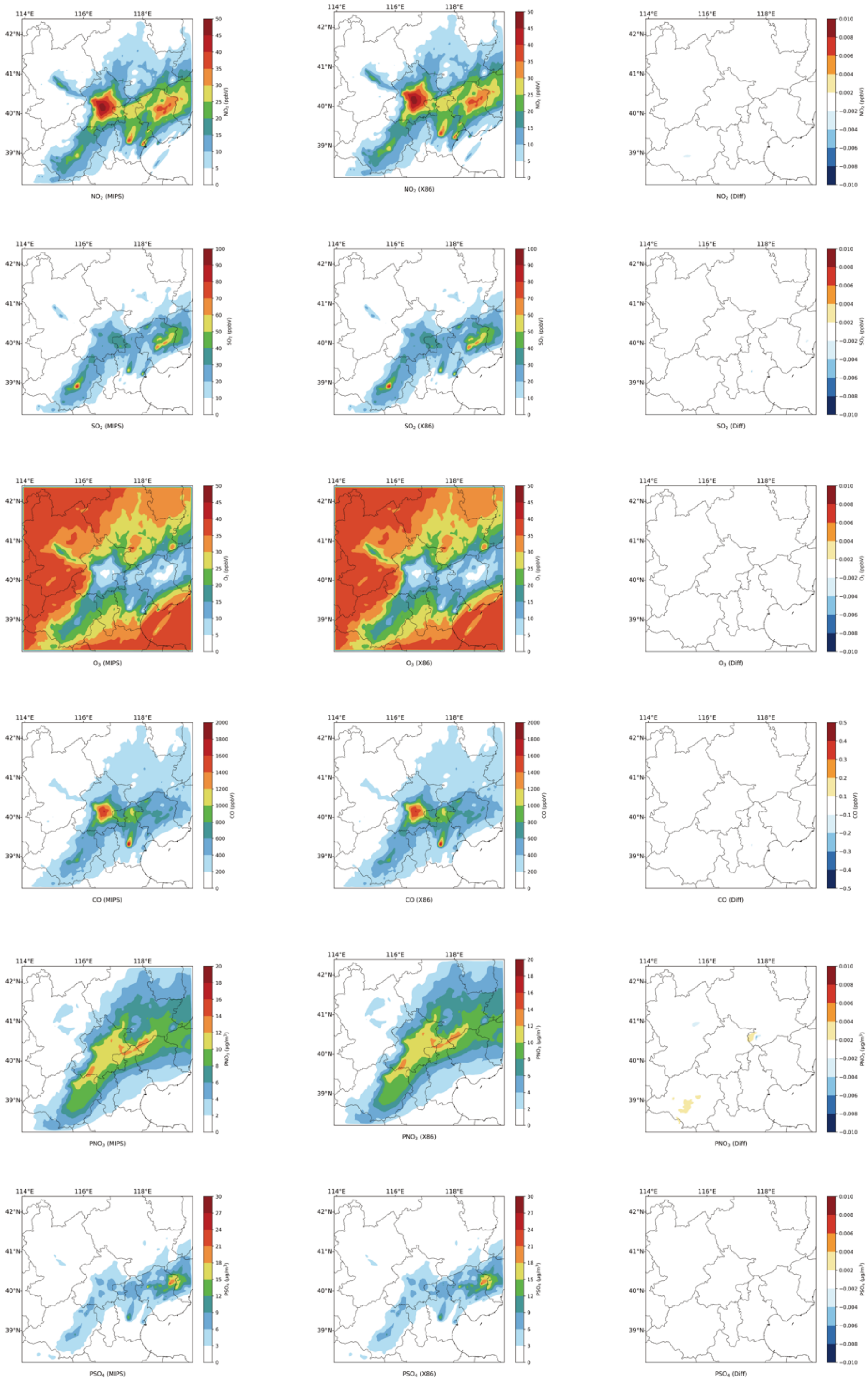

Figure 5. Spatial distribution of NO_2, SO_2, O_3, CO, PNO_3 and PSO_4 from CAMx on MIPS and benchmark platform. Left column, MIPS platform. Middle, the X86 platform. Right, the differences between the MIPS and benchmark(X86) platform.

As shown in Figure 6, the scatter plots between the two platform, it can be seen that for the total of 22,765 grids within the 145x157 simulation domain, the root mean square errors (RMSEs) of the six species between the MIPS platform and benchmark platform are close to 0.001, which is essentially 0. The linear regression model was used to fit the scatters, and the regression slopes for each species are nearly 1, with intercepts close to 0, and the R2 values used for the goodness of fit are nearly 1. The fitted lines closely coincide with the "y=x" line, indicating that the differences between the MIPS and X86 platform for each species are minimal to negligible.

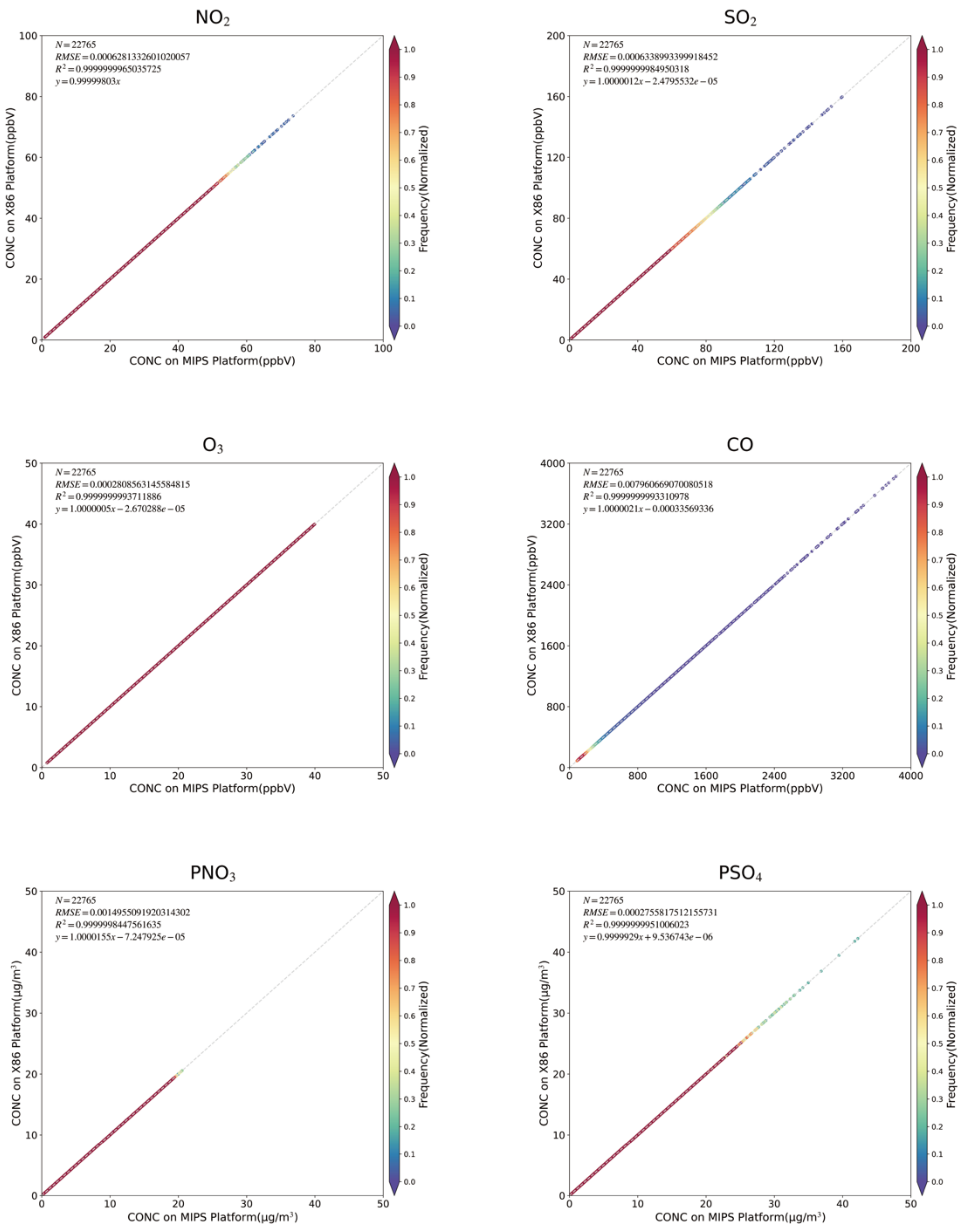

Figure 6. Scatter of grid concentrations for NO_2, SO_2, O_3, CO, PNO_3 and PSO_4 from CAMx on the MIPS and benchmark platform. The density of scatters is represented by

the colors.

Figure 7 is the boxplots which show the absolute errors (AE) and relative errors (RE) of the six species between MIPS and benchmark platform. According to Figure 7, the absolute errors of the six species are generally in the range of $\pm10^{-3}$ ppbv (parts per billion by volume; the unit of NO_2, SO_2, O_3 and CO concentration) or μg m^{-3}(the unit of particle composition PNO_3 and PSO_4), and the relative errors are generally in the range of ±0.01%. Specially for CO, it exhibits more pronounced AEs compared to other species. In some grid boxes, the AEs between MIPS and benchmark platform exceed the range of $\pm10^{-3}$ ppbv, but they remain in the range of $\pm10^{-2}$ ppbv. In summary, there are some errors between the results of the modeling system on the MIPS and benchmark platform during the porting process. However, these errors are relatively minor compared to the numerical values. The reasons are attributed to the differences in the CPU architecture and compiler characteristics between the two platforms, such as data operations and precision running on different CPUs, which are primarily responsible for the observed errors.

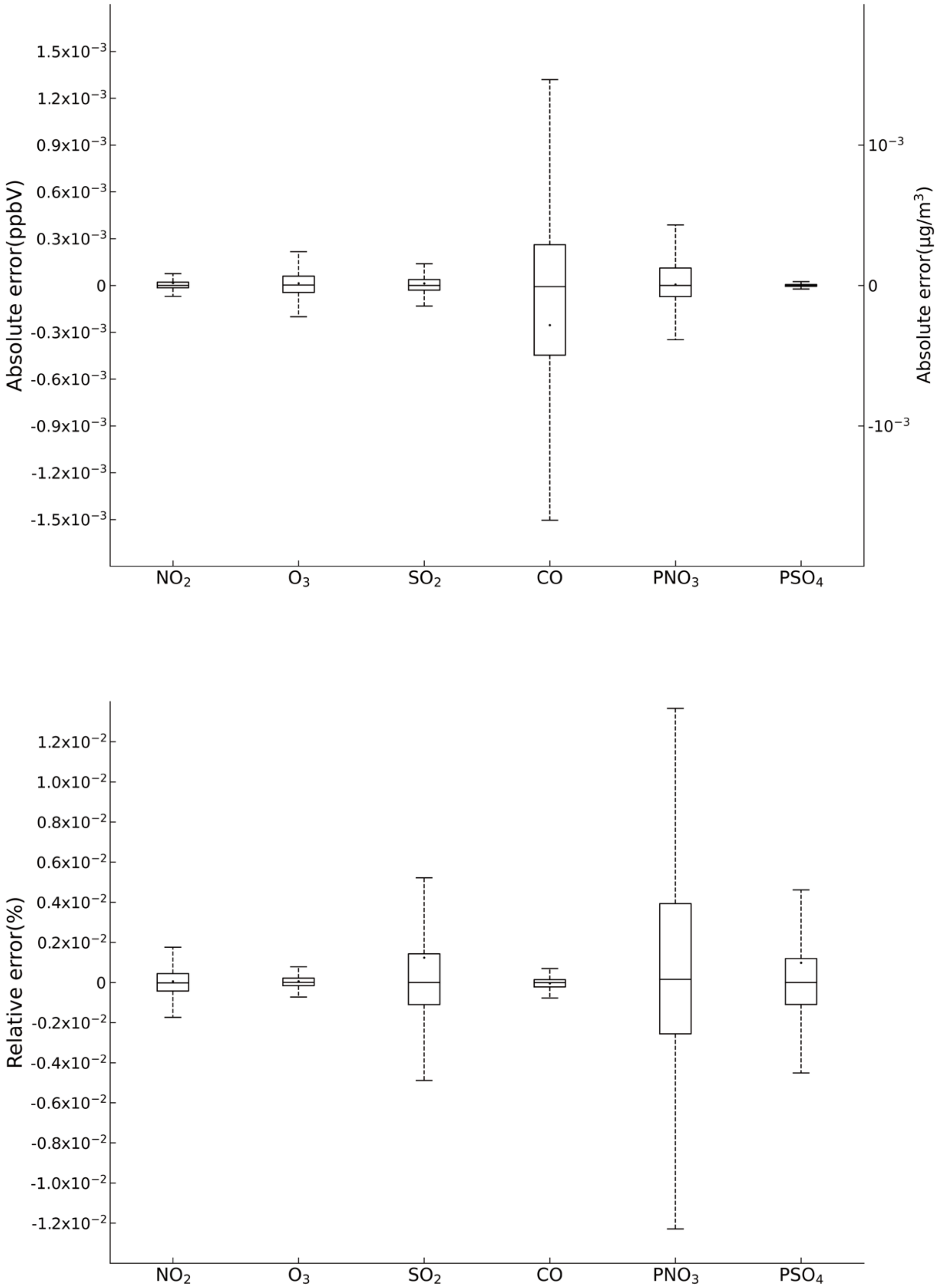

Figure 7. The absolute errors and relative errors for NO_2, SO_2, O_3, CO, PNO_3 and PSO_4 concentration in all grids between the MIPS and benchmark platform.

Additionally, random grids in the domain were selected to assess the precision of simulation results in localized regions. The positions of these grids were determined based on 32 observation stations in Beijing, and the nearest grid was determined using the Euclidean Shortest Distance in the domain. The station map is presented in Figure S1 in the Supplement. The Taylor diagram is used to assess the precision of concentrations for six species near the observation stations, and the scatters representing the six species at 32 stations are highly overlapping. Statistical parameters used in the Taylor diagram, such as the correlation coefficient (R) approaching 1, normalized standard deviation (NSD) and normalized root mean square error (NRMSE) approaching 0, indicate high precision of the simulation results at specific stations on the MIPS platform.

4.2 Validation of the temporal distribution from the two platform

The time series of computational differences also be evaluated in this study. Random grid in the domain was selected to examine the hourly concentrations of the six species. Taking the example of the Beijing Olympic Center station (116.40ºE, 39.99ºN) from the National Standard Air Quality (NSAQ) stations, the time series of hourly concentrations in the grid of the Beijing Olympic Center station and relative errors between the MIPS and benchmark platform over the 72-hour period were shown in Figure 8. As shown in Figure 8, it can be seen that the time series of the air pollutant concentrations were highly consistent between the two platforms. In the 72-hour period, the relative errors for NO_2, SO_2, CO and PSO_4 remain in ±0.025%. For PNO_3, the relative errors remain in ±0.05%, and for O_3, they remain in ±0.1%. This indicates that the errors caused by different architectures are within a reasonable range.

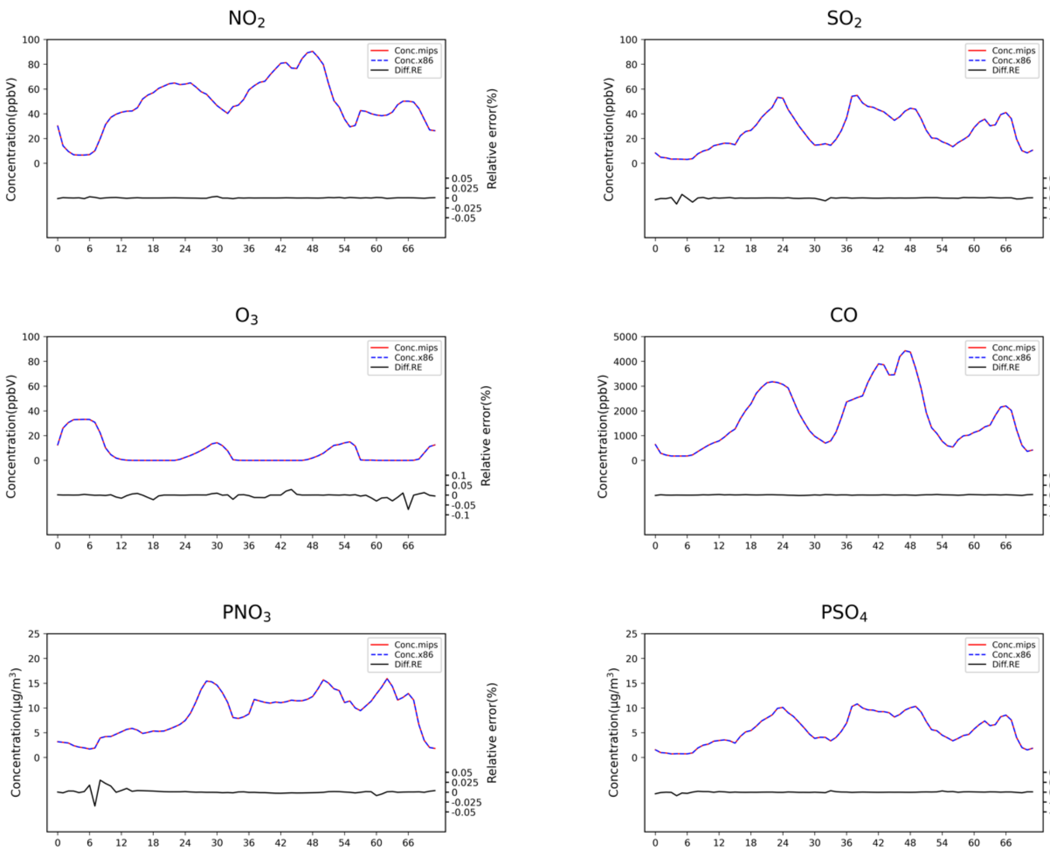

Figure 8. Time-series of NO_2, SO_2, O_3, CO, PNO_3 and PSO_4 concentrations and its relative errors (RE) at the Beijing Olympic Sports Center site between the MIPS and X86 platform. The red solid line and the blue dashed line, the CAMx model results on MIPS platform and X86 platform. The black solid line shows the relative errors (RE) between the MIPS and X86 platform.

Figure 9 shows the time series of the concentration and their statistical indicators, MAE, RMSE, and MAPE during the 72-hour simulation. As show in the figure, for NO_2, SO_2, O_3, and PSO_4, the MAEs are all below 10^{-3} ppbv (μg m^{-3}), and the RMSEs are all below 10^{-3}. The MAEs for CO and PNO_3 are below 10^{-2} ppbv (μg m^{-3}), and the RMSEs for PNO_3 are below 10^{-2}, while the RMSEs for CO are below 10^{-1}. This is because that PNO_3 and CO have relatively higher background concentrations compared to the other species. The MAPE of PNO_3 concentration mainly ranging in 0-0.5%, while the MAPE of CO concentration has the lowest values below 0.001%, and the other species are in the range of 0-0.01%. Overall, the above time-series analysis verifies the accuracy and stability of the modeling system on the MIPS platform.

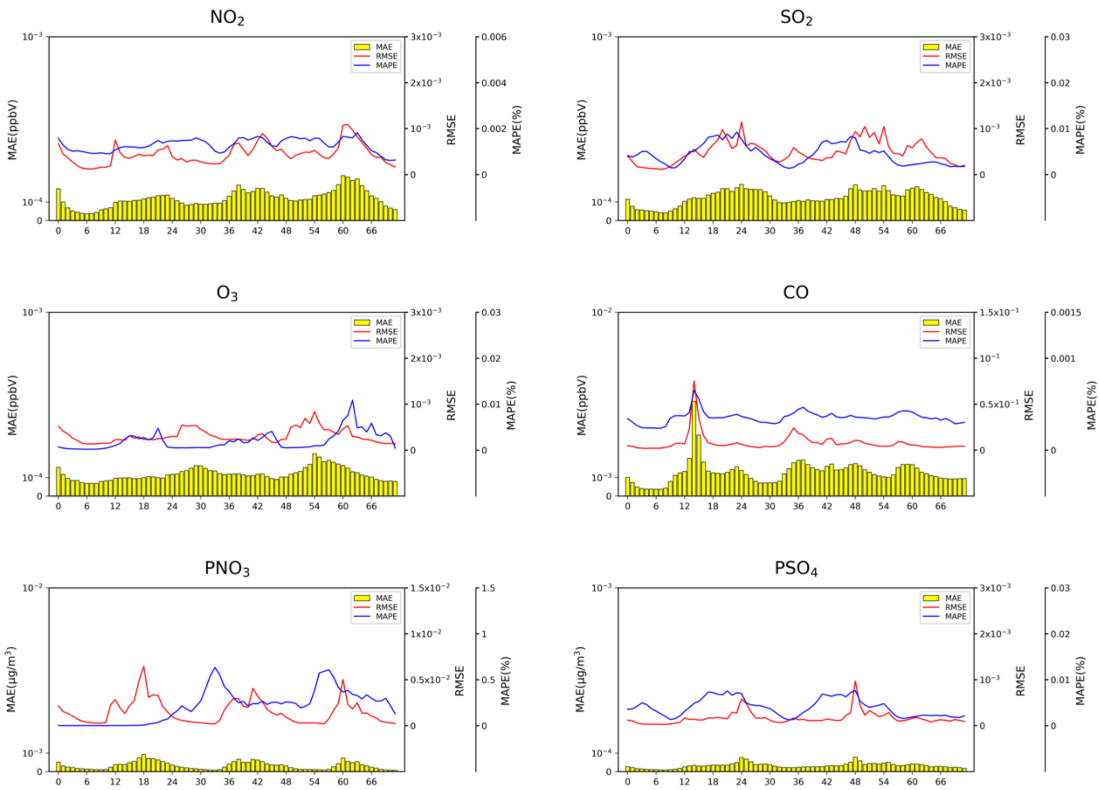

Figure 9. Time series of MAEs, RMSEs and MAPEs for NO_2, SO_2, O_3, CO, PNO_3 and PSO_4 concentration in the 72h simulation. The yellow bar, the MAE. The red lines, RMSE, the blue lines, MAPE.

In this study, the evaluation method proposed by Wang et al. (2021) was also used to assess the scientific applicability of the model results on the MIPS platform. The Root Mean Square Errors (RMSEs) for NO_2, SO_2, O_3, CO, PNO_3 and PSO_4 concentration between the MIPS and benchmark platform were computed, along with the standard deviations (stds) used to describe the spatial variation of species, and the ratio of RMSE to std, as shown in Table 6. The differences of the four species between the two platforms are negligible compared to their own spatial variations. Therefore, the results on the MIPS platform meet the accuracy requirements for research purpose.

Table 6. RMSE, std, RMSE/std for NO_2, SO_2, O_3, CO, PNO_3 and PSO_4.

	Differences in results	Spatial variation	RMSE/std
	RMSE	**std**	
NO_2	6.3×10^{-7}	0.01	5.9×10^{-5}

O_3	2.8×10^{-7}	0.01	2.5×10^{-5}
SO_2	6.3×10^{-7}	0.02	3.9×10^{-5}
CO	7.9×10^{-6}	0.30	2.6×10^{-5}
PNO_3	1.5×10^{-3}	3.8	3.9×10^{-4}
PSO_4	2.7×10^{-4}	3.9	6.9×10^{-5}

In fact, the differences in model results cannot be completely eliminated, primarily due to the varying CPU architectures and compilers. In the practical applications, compared with the errors arising from the inherent uncertainties of the modeling system and the input data, the differences of model results between different platforms can even be considered negligible. The comprehensive analysis demonstrates that the results of the WRF-CAMx modeling system on the MIPS CPU platform are reasonable.

5 The evaluation about computational performance

Scientific computing involves a significant amount of floating-point operations, and the floating-point computational capability is a crucial indicator for CPU performance. In this study, the simulation case was configured to conduct parallel computing tests on the MIPS, LoongArch and benchmark platform. These tests included assessing the CPU's single-core performance with the non-parallel model and the platform's parallel performance with the parallel model using multiple processes. The time of CAMx model running simulation case for 24 hours in the modeling system are shown in Figure 10. From the figure, it can be observed that under single-core conditions, the computing capability of the MIPS platform for CAMx is approximately one-third of the X86 benchmark platform, and the LoongArch platform is slightly lower than the X86 benchmark platform.

It's worth noting that the simulation time of the CAMx model for running with two processes in parallel and running in non-parallel remains approximately consistent. This is because the MPI used in CAMx is designed using a "master/slave" parallel processing approach, and a process is allocated for input/output and message communication during the runtime (Cao K et al., 2023). This process doesn't perform any simulation in the model. Therefore, the time required for parallelism of two processes is comparable to the non-parallelism, and in some cases, it might even be slightly longer due to the overhead of MPI communication. Compared to non-parallel, the speedup of the MIPS platform with four-process parallelism using MPICH3 is approximately 2.8, while using OpenMP is about 2.9, and the speedup of the LoongArch platform with four-process parallelism using MPICH3 is approximately 2.8, while using OpenMP is about 2.9. For the X86 benchmark platform, running with four processes in parallel using MPICH3 has a speedup of approximately 2.7.

Additionally, the performance of the MIPS platform significantly decreases when the number of parallel processes exceeds 4. This is because the modeling system involves compute-intensive tasks. The Loongson 3A4000 CPU has four cores, and when the number of processes called by MPI matches the number of CPU cores, the CPU utilization can approach 100%. Further increasing the number of processes, the cores will compete for CPU resources, resulting in additional overhead and reduced computational efficiency. As for LoongArch platform, the performance slightly decreases when the number of parallel processes exceeds 4. The Loongson 3A6000 CPU has four physical cores and eight logical cores, and when the number of processes called by MPI matches the number of physical cores, the computational load is evenly distributed across each core. Although the Loongson 3A6000 supports hyper-threading, further increasing the number of processes, CPU starts to schedule logical cores to allocate computational load. Thread scheduling will result in additional overhead and reduced computational efficiency. This explains why the elapsed time is slightly higher when CAMx running with 5 parallel processes compared to 4 parallel processes as shown in the section 2 of Supplementary Material.

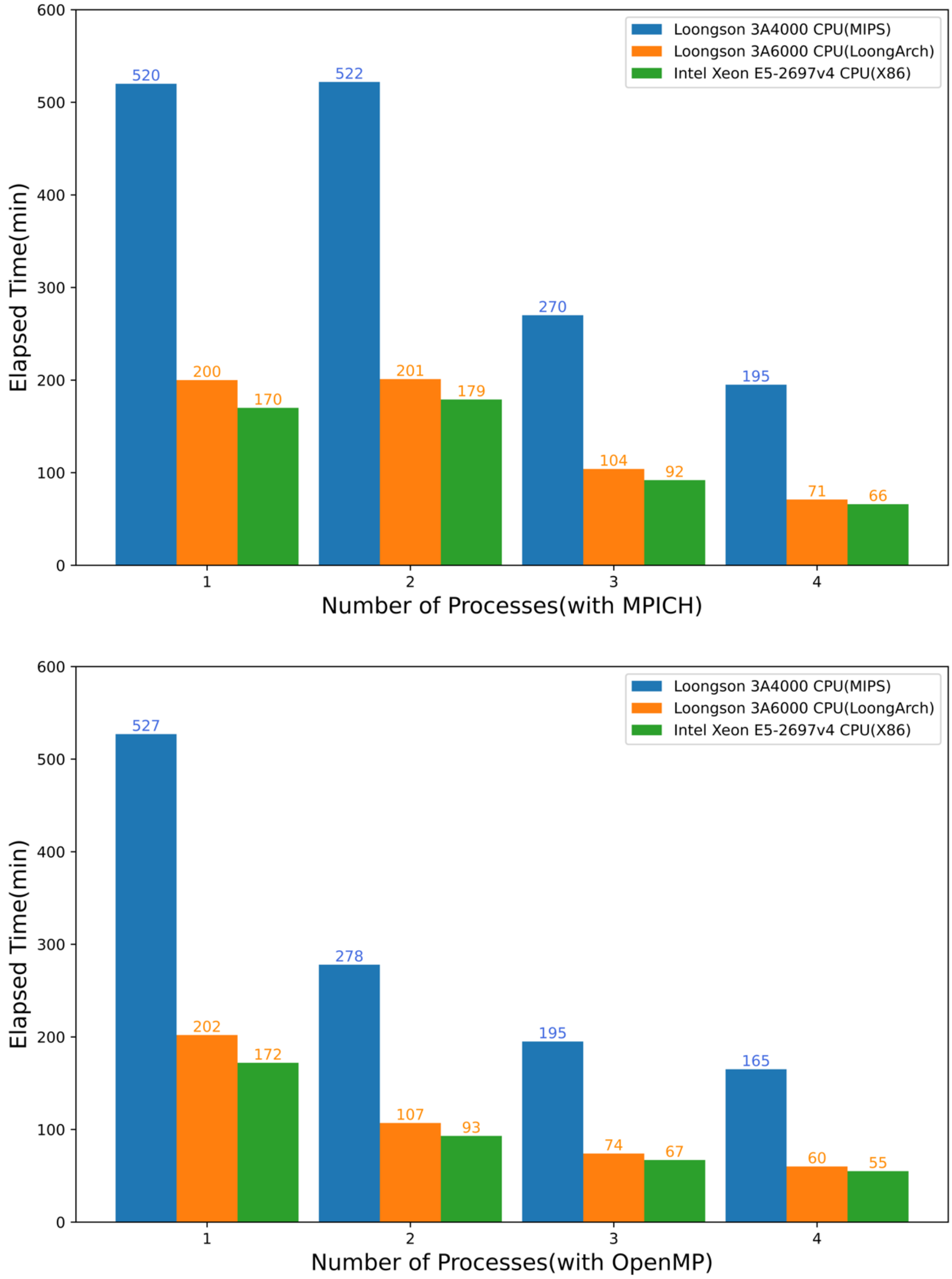

Figure 10. Elapsed time of CAMx model running simulation case with MPICH and OpenMP for 24 hours on the MIPS, LoongArch and benchmark platforms.

In the recent years, the Loongson CPUs have been continuously upgraded. Compared to the previous generations of products, the performance of Loongson CPUs has shown significant improvement. Wu et al. (2019) simulated a nested domain covering Beijing for 48 hours using the MM5 model on the Loongson 3A quad-core CPU platform. The results showed that the computational capacity of the Loongson 3A platform for the MM5 model is approximately equivalent to around 1/12 of the Intel Core 2 Q8400 quad-core CPU, which was released in the same year. In the study of Luo et al. (2011), a comparison between Loongson 3A and Intel i5 was made by running NPB benchmark on each platform. The results shows that the performance of the 3A is nearly one-tenth of that of the i5. The rapid development of Loongson CPUs has provided a strong hardware foundation for the application of numerical simulation and scientific computing on MIPS and LoongArch architecture CPU platforms. Based on the performance evaluation of WRF-CAMx modeling system on Loongson 3A4000 and Loongson 3A6000 platform, it could be found that the computing capability nearly tripled while maintaining similar power consumption. The adaptation and optimization of the models based on RISC CPUs will also be an important research direction in the future. Many factors influencing parallel performance, such as computing scale, I/O, multiprocessor, etc., will be considered to evaluate on platforms with stronger performance and more processors in the future.

6 Conclusion

This study describes the application of the WRF-CAMx model on the MIPS CPU platform. The platform used in this study is Loongson 3A4000 quad-core CPU with the main frequency of 1.8-2.0GHz, which can offer a peak operational speed of 128GFlops. It is equipped with the MIPS GNU compiler. The benchmark platform used the Intel Xeon E5-2697 v4 CPU along with the same version of X86 GNU compiler. Based on the characteristics of CPU architecture and compiler, this study has successfully completed the construction of runtime environment for the WRF-CAMx modeling system. The application of an air quality modelling system based on WRF-CAMx was successfully tested using a 72-hour simulation case in the Beijing-Tianjin-Hebei region.

The results showed that the spatial distribution of the meteorological variables and air pollutant species was nearly identical, with relative errors in the range of ±0.1%.

Statistically, the maximum MAEs of major species ranged from 10^{-3} to 10^{-2} ppbv (μg m^{-3}), the maximum RMSEs ranged from 10^{-2} to 10^{-1} ppbv (μg m^{-3}), and the MAPEs remained within 0.5%, that the differences caused by the architectures and compilers were within a reasonable range. Simulating a 2h-case with four parallel processes using MPICH, CAMx takes about 15.2min on Loongson 3A4000 CPU and 4.8 min on Intel Xeon E5-2697 v4 CPU. In terms of single-core CPU performance, the single-core computing capability of Loongson 3A4000 CPU for the WRF-CAMx modeling system is about one-third of Intel Xeon E5-2697 v4 CPU.

Currently, Loongson Technology has focused on the LoongArch architecture and it has been used in the latest product. It is foreseeable that the LoongArch architecture will lead to more significant performance improvements. In the future, as the numerical models become more complex and computational scales become larger, more models will be tested on high-performance computing platforms equipped with the LoongArch architecture CPUs.

Code and data availability. The source codes of CAMx version 6.10 are available at https://camx-wp.azurewebsites.net/download/source (ENVIRON, 2023). The datasets related to this paper and the binary executable files of CAMx for MIPS and LoongArch CPUs are available online via ZENODO (https://doi.org/10.5281/zenodo.10722127).

Supplement. The supplement related to this article is available on-line.

Author contributions. ZB and QW conducted the simulation and prepared the materials. QW planned and organized the project. ZB and QW completed the porting and application of the model for MIPS and LoongArch CPUs. YS collected and prepared the emission data for the simulation. ZB, QW, KC, and HC participated in the discussion.

Acknowledgements. The National Key R&D Program of China (2020YFA0607804) and the Beijing Advanced Innovation Program for Land Surface funded this work. The

research is supported by the High Performance Scientific Computing Center (HSCC) of Beijing Normal University.

Competing interests. The contact author has declared that none of the authors has any competing interests.

References

Amer, A., Balaji, P., Bland, W., Gropp, W., Guo, Y., Latham, R., Lu, H., Oden, L., Pena, A. J., Raffenetti, K., Seo, S., Si, M., Thakur, R., Zhang, J., and Zhao, X.: MPICH User's Guide Version 3.4, available at: https://www.mpich.org/static/downloads/3.4/mpich-3.4-userguide.pdf , 2021.

Appel, K. W., Napelenok, S. L., Foley, K. M., Pye, H. O. T., Hogrefe, C., Luecken, D. J., Bash, J. O., Roselle, S. J., Pleim, J. E., Foroutan, H., Hutzell, W. T., Pouliot, G. A., Sarwar, G., Fahey, K. M., Gantt, B., Gilliam, R. C., Heath, N. K., Kang, D., Mathur, R., and Schwede, D. B.: Description and evaluation of the Community Multiscale Air Quality (CMAQ) modeling system version 5.1, Geoscientific Model Development, 10, 1703–1732, https://doi.org/10.5194/gmd-10-1703-2017, 2017.

Appel, K. W., Bash, J. O., Fahey, K. M., Foley, K. M., Gilliam, R. C., Hogrefe, C., Hutzell, W. T., Kang, D., Mathur, R., Murphy, B. N., Napelenok, S. L., Nolte, C. G., Pleim, J. E., Pouliot, G. A., Pye, H. O. T., Ran, L., Roselle, S. J., Sarwar, G., Schwede, D. B., Sidi, F. I., Spero, T. L., and Wong, D. C.: The Community Multiscale Air Quality (CMAQ) model versions 5.3 and 5.3.1: system updates and evaluation, Geoscientific Model Development, 14, 2867–2897, https://doi.org/10.5194/gmd-14-2867-2021, 2021.

Bai, X., Tian, H., Liu, X., Wu, B., Liu, S., Hao, Y., Luo, L., Liu, W., Zhao, S., Lin, S., Hao, J., Guo, Z., and Lv, Y.: Spatial-temporal variation characteristics of air pollution and apportionment of contributions by different sources in Shanxi province of China, Atmospheric Environment, 244, 117926, https://doi.org/10.1016/j.atmosenv.2020.117926, 2021.

Cao, K., Wu, Q., Wang, L., Wang, N., Cheng, H., Tang, X., Li, D., and Wang, L.: GPU-HADVPPM V1.0: a high-efficiency parallel GPU design of the piecewise parabolic method (PPM) for horizontal advection in an air quality model (CAMx V6.10), Geosci. Model Dev., 16, 4367–4383, https://doi.org/10.5194/gmd-16-4367-2023, 2023.

Chen, H. S., Wang, Z. F., Li, J., Tang, X., Ge, B. Z., Wu, X. L., Wild, O., and Carmichael, G. R.: GNAQPMS-Hg v1.0, a global nested atmospheric mercury transport model: model description, evaluation and application to trans-boundary transport of Chinese anthropogenic emissions, Geoscientific Model Development, 8, 2857–2876, https://doi.org/10.5194/gmd-8-2857-2015, 2015.

George, A. D.: An overview of RISC vs. CISC, in: [1990] Proceedings. The Twenty-Second Southeastern Symposium on System Theory, The Twenty-Second Southeastern Symposium on System Theory, Cookeville, TN, USA, 436–438, https://doi.org/10.1109/SSST.1990.138185, 1990.

Hennessy, J., Jouppi, N., Przybylski, S., Rowen, C., Gross, T., Baskett, F., and Gill, J.: MIPS: A microprocessor architecture, SIGMICRO Newsl., 13, 17–22, https://doi.org/10.1145/1014194.800930, 1982.

Hu, W., Wang, J., Gao, X., Chen, Y., Liu, Q., and Li, G.: Godson-3: A Scalable Multicore RISC Processor with x86 Emulation, IEEE Micro, 29, 17–29, https://doi.org/10.1109/MM.2009.30, 2009.

Hu, W., Zhang, Y., and Fu, J.: An introduction to CPU and DSP design in China, Sci. China Inf. Sci., 59, 1–8, https://doi.org/10.1007/s11432-015-5431-6, 2016.

Hu, W., Gao, X., and Zhang, G.: Building the softw are ecosystem for the Loongson instruction set architecture, Information and Communications Technology and Policy, 43–48, 2022 (in Chinese).

Hu, W.-W., Gao, Y.-P., Chen, T.-S., and Xiao, J.-H.: The Godson Processors: Its Research, Development, and Contributions, J. Comput. Sci. Technol., 26, 363–372, https://doi.org/10.1007/s11390-011-1139-2, 2011.

Intel Inc.: Intel® 64 and IA-32 Architectures Software Developer's Manual, Volume 1: Ba sic Architecture, available at: https://www.intel.com/content/www/us/en/developer/articles/technical/intel-sdm.html, 2023.

Li, L., Chen, Z., and Wang, S.: Power Consumption and Analysis of Server Based on Loongson CPU No. 3, Information Technology & Standardization, 46–50, 2014 (in Chinese).

Liu, Y., Ye, K., and Xu, C.-Z.: Performance Evaluation of Various RISC Processor Systems: A Case Study on ARM, MIPS and RISC-V, in: Cloud Computing – CLOUD 2021, Cham, 61–74, https://doi.org/10.1007/978-3-030-96326-2_5, 2022.

Luo, Q., Kong, C., Cai, Y., and Liu, G.: Performance Evaluation of OpenMP Constructs and Kernel Benchmarks on a Loongson-3A Quad-Core SMP System, in: 2011 12th International Conference on Parallel and Distributed Computing, Applications and Technologies, 2011 12th International Conference on Parallel and Distributed Computing, Applications and Technologies, 191–196, https://doi.org/10.1109/PDCAT.2011.66, 2011.

Mallach, E. G.: RISC: Evaluation and Selection, Journal of Information Systems Management, 8, 8–16, https://doi.org/10.1080/07399019108964978, 1991.

Michalakes, J., Chen, S., Dudhia, J., Hart, L., Klemp, J., Middlecoff, J., and Skamarock, W.: Development of a next-generation regional weather research and forecast model, in: Developments in Teracomputing, WORLD SCIENTIFIC, 269–276, https://doi.org/10.1142/9789812799685_0024, 2001.

MIPS Technology Inc.: MIPS Architecture For Programmers Volume I-A, available at: https://www.mips.com/products/architectures/mips64, 2014.

Pepe, N., Pirovano, G., Lonati, G., Balzarini, A., Toppetti, A., Riva, G. M., and Bedogni, M.: Development and application of a high resolution hybrid modelling system for the evaluation of urban air quality, Atmospheric Environment, 141, 297–311, https://doi.org/10.1016/j.atmosenv.2016.06.071, 2016.

Powers, J. G., Klemp, J. B., Skamarock, W. C., Davis, C. A., Dudhia, J., Gill, D. O., Coen, J. L., Gochis, D. J., Ahmadov, R., Peckham, S. E., Grell, G. A., Michalakes, J., Trahan, S., Benjamin, S. G., Alexander, C. R., Dimego, G. J., Wang, W., Schwartz, C. S., Romine, G. S., Liu, Z., Snyder, C., Chen, F., Barlage, M. J., Yu, W., and Duda, M. G.: The Weather Research and Forecasting Model: Overview, System Efforts, and Future Directions, Bulletin of the American Meteorological Society, 98, 1717–1737, https://doi.org/10.1175/BAMS-D-15-00308.1, 2017.

RAMBOLL ENVIRON Inc.: CAMx User's Guide Version 6.1, available at: https://camx-wp.azurewebsites.net/Files/CAMxUsersGuide_v6.10.pdf, 2014.
Shi, Z.: Technology comparison and research of RISC and CISC, China Science and Technology Information, 131–132, 2008 (in Chinese).
Skamarock, C., Klemp, B., Dudhia, J., Gill, O., Liu, Z., Berner, J., Wang, W., Powers, G., Duda, G., Barker, D., and Huang, X.: A Description of the Advanced Research WRF Model Version 4, https://doi.org/10.5065/1dfh-6p97, 2019.
Sun Y.: Research on the contribution of soil fugitive dust in Beijing based on satellite identification and numerical simulation techology, Master, Beijing Normal University, https://etdlib.bnu.edu.cn, 2022a.
Sun, Y., Wu, Q., Wang, L., Zhang, B., Yan, P., Wang, L., Cheng, H., Lv, M., Wang, N., and Ma, S.: Weather Reduced the Annual Heavy Pollution Days after 2016 in Beijing, Sola, 18, 135–139, https://doi.org/10.2151/sola.2022-022, 2022b.
The HDF Group: HDF5 User's Guide Version 1.1, available at: https://portal.hdfgroup.org/display/HDF5/HDF5+User+Guides, 2019.
UCAR/Unidata: NetCDF User's Guide Version 1.1, available at: https://docs.unidata.ucar.edu/nug , 2021.
Wang, H., Lin, J., Wu, Q., Chen, H., Tang, X., Wang, Z., Chen, X., Cheng, H., and Wang, L.: MP CBM-Z V1.0: design for a new Carbon Bond Mechanism Z (CBM-Z) gas-phase chemical mechanism architecture for next-generation processors, Geoscientific Model Development, 12, 749–764, https://doi.org/10.5194/gmd-12-749-2019, 2019.
Wang, K., Gao, C., Wu, K., Liu, K., Wang, H., Dan, M., Ji, X., and Tong, Q.: ISAT v2.0: an integrated tool for nested-domain configurations and model-ready emission inventories for WRF-AQM, Geoscientific Model Development, 16, 1961–1973, https://doi.org/10.5194/gmd-16-1961-2023, 2023.
Wang, P., Jiang, J., Lin, P., Ding, M., Wei, J., Zhang, F., Zhao, L., Li, Y., Yu, Z., Zheng, W., Yu, Y., Chi, X., and Liu, H.: The GPU version of LASG/IAP Climate System Ocean Model version 3 (LICOM3) under the heterogeneous-compute interface for portability (HIP) framework and its large-scale application, Geosci. Model Dev., 14, 2781–2799, https://doi.org/10.5194/gmd-14-2781-2021, 2021.
Wang, S., Li, L., and Chen, Z.: The Test and Analysis on Memory Access Performance Based on Loongson CPU, Information Technology & Standardization, 32–36, 2014 (in Chinese).
Wang, Z., Xie, F., Wang, X., An, J., and Zhu, J.: Development and Application of Nested Air Quality Prediction Modeling System, Chinese Journal of Atmospheric Sciences, 778–790, http://dx.doi.org/10.3878/j.issn.1006-9895.2006.05.07, 2006.
Wu, Q. and Cheng, H.: Transplantation and application of mesoscale mode on Loongson CPU platform, Journal of Beijing Normal University (Natural Science), 55, 11–18, https://doi.org/10.16360/j.cnki.jbnuns.2019.01.002, 2019.
Wu, Q., Xu, W., Shi, A., Li, Y., Zhao, X., Wang, Z., Li, J., and Wang, L.: Air quality forecast of PM10 in Beijing with Community Multi-scale Air Quality Modeling (CMAQ) system: emission and improvement, Geoscientific Model Development, 7, 2243–2259, https://doi.org/10.5194/gmd-7-2243-2014, 2014.
Wu, Y., Xu, G., Zhao, Y., and Tan, Y.: Parallel Processing on WRF Meteorological Data Using MPICH, in: 2012 Sixth International Conference on Internet Computing for Science and

Engineering, 2012 Sixth International Conference on Internet Computing for Science and Engineering, titleTranslation:, 262–265, https://doi.org/10.1109/ICICSE.2012.12, 2012.

Xiao, H., Wu, Q., Yang, X., Wang, L., and Cheng, H.: Numerical study of the effects of initial conditions and emissions on PM2.5 concentration simulations with CAMx v6.1: a Xi'an case study, Geoscientific Model Development, 14, 223–238, https://doi.org/10.5194/gmd-14-223-2021, 2021.

Yang, X., Xiao, H., Wu, Q., Wang, L., Guo, Q., Cheng, H., Wang, R., and Tang, Z.: Numerical study of air pollution over a typical basin topography: Source appointment of fine particulate matter during one severe haze in the megacity Xi'an, Science of The Total Environment, 708, 135213, https://doi.org/10.1016/j.scitotenv.2019.135213, 2020.

Zhang, Y., Bocquet, M., Mallet, V., Seigneur, C., and Baklanov, A.: Real-time air quality forecasting, part I: History, techniques, and current status, Atmospheric Environment, 60, 632–655, https://doi.org/10.1016/j.atmosenv.2012.06.031, 2012.

Zhang, Z., Wang, X., Cheng, S., Guan, P., Zhang, H., Shan, C., and Fu, Y.: Investigation on the difference of PM2.5 transport flux between the North China Plain and the Sichuan Basin, Atmospheric Environment, 271, 118922, https://doi.org/10.1016/j.atmosenv.2021.118922, 2022.

Zhen, J., Guan, P., Yang, R., and Zhai, M.: Transport matrix of PM2.5 in Beijing-Tianjin-Hebei and Yangtze River Delta regions: Assessing the contributions from emission reduction and meteorological conditions, Atmospheric Environment, 304, 119775, https://doi.org/10.1016/j.atmosenv.2023.119775, 2023.

Zhi, Y. and Xu, J.: Android transplantation and analysis based on Loongson, in: 2012 International Conference on Information Management, Innovation Management and Industrial Engineering, 2012 International Conference on Information Management, Innovation Management and Industrial Engineering, 59–61, https://doi.org/10.1109/ICIII.2012.6339777, 2012.